A&A 421, 595–601 (2004)
DOI: 10.1051/0004-6361:20035735

Astronomy & Astrophysics

Deprojecting spiral galaxies using Fourier analysis. Application to the Ohio sample★

C. García-Gómez[1], C. Barberà[1], E. Athanassoula[2], A. Bosma[2], and L. Whyte[3]

[1] DEIM, Campus Sescelades, Avd. dels Països Catalans 26, 43007 Tarragona, Spain
[2] Observatoire de Marseille, 2 place Le Verrier, 13248 Marseille Cedex 04, France
[3] School of Physics and Astronomy, University of Nottingham, Nottingham NG7 2RD, UK

Received 24 November 2003 / Accepted 7 April 2004

Abstract. We use two new methods developed recently (Barberà et al. 2004, A&A, 415, 849), as well as information obtained from the literature, to calculate the orientation parameters of the spiral galaxies in the Ohio State University Bright Galaxy Survey. We compare the results of these methods with data from the literature, and find in general good agreement. We provide a homogeneous set of mean orientation parameters which can be used to approximately deproject the disks of the galaxies and facilitate a number of statistical studies of galaxy properties.

Key words. galaxies: structure – galaxies: spiral

1. Introduction

The accurate determination of the deprojection angles of a spiral galaxy is a necessary first step before one can study quantitatively its morphology, photometry or kinematics. These angles are the position angle (hereafter PA), which is the angle between the line of nodes of the projected image and the north, measured towards the east, and the inclination angle (hereafter IA), which is the angle between the perpendicular to the plane of the galaxy and the line of sight.

In this paper we use the two methods based on the Fourier transform of galactic images developed recently (Barberà et al. 2004, hereafter BAG) and combine them with information obtained from different sources in the literature to obtain accurate values of the deprojection angles of the Ohio State University Bright Spiral Galaxy Survey (hereafter OSU) sample of bright galaxies. We will use this information in subsequent papers to deproject the galaxy images so as to be able to study the spiral structure in disc galaxies by decomposing each image with the help of bidimensional Fourier transforms.

The OSU survey has been described thoroughly in Eskridge et al. (2002) and will not be discussed further here. The Early Data Release (20 June 2002) is a magnitude limited sample containing 205 disc galaxies with Hubble types $T \geq 0$, apparent magnitudes $M_B \leq 12$ and diameters $D \leq 6\farcm5$. As in the preceding paper (BAG), we have concentrated on the galaxies with Hubble types $2 \leq T \leq 7$ for which the Fourier methods can be usefully applied. This brings our sample to a total of 158 galaxies which, when combined with the disc galaxies of the Frei et al. (1996) sample, will constitute a sample of about 200 galaxies with different Hubble types and with information in different colour bands on which we will base our subsequent studies on spiral structure in spiral galaxies.

2. Deprojection methods

The determination of the deprojection angles of spiral galaxies can be made using different methods, usually based either on the photometry, or on the kinematics. In the photometric methods ellipses are fitted to the outer isophotes of the images. The axis ratio of the outer ellipses is given as a measure of the IA, while the direction of the major axis of the ellipse gives the PA. The observation of the gas kinematics within the disc, with the determination of two dimensional velocity fields, is another commonly used method. It is necessary to make the assumption that the emission comes from material in a thin disc in circular motion around the center. The selected PA and IA angles are those which minimize the departures from such a flow. This method is the most reliable one for the determination of the PA of galaxies near face on.

Several other methods can be found in the literature. For instance, Danver (1942) used a special display table to rotate the galaxy images until they looked approximately circular. Grøsbol (1985) used a one dimensional Fourier transform of the intensity distribution in the outer parts of galaxy discs and adopted the deprojection angles that minimized the bisymmetric ($m = 2$) Fourier coefficient. Comte et al. (1979)

Send offprint requests to: C. García-Gómez,
e-mail: `cgarcia@etse.urv.es`

★ Table 1 is only available in electronic form at the CDS via anonymous ftp to `cdsarc.u-strasbg.fr (130.79.128.5)` or via `http://cdsweb.u-strasbg.fr/cgi-bin/qcat?J/A+A/421/595` used the distribution of HII regions in the $\ln(r) - \theta$ plane to fit straight lines to the arms, under the hypothesis that they are well described by logarithmic spirals. Two dimensional Fourier analysis, similar to the methods presented in BAG, has also been used previously to determine the deprojection angles. Considère & Athanassoula (1982) used the HII region distribution, selecting the angles that maximized the signal-to-noise ratio in the $m = 2$ component, and Considère & Athanassoula (1988), applied the same criterion to galaxy images. Iye et al. (1982) used an image of NGC 4254 and selected the angles that maximize the axisymmetric component. Finally, García-Gómez & Athanassoula (1991) and García-Gómez et al. (2002) also used HII region distributions and maximized the axisymmetric components. These authors also used a second method selecting the deprojection angles that make the HII region distribution most uniform with azimuth.

In BAG we introduced two new methods, again based on the Fourier transforms, which are closely related to the two methods used by García-Gómez et al. (2002) for HII region distributions. Let $I(u, \theta)$ be the image of the galaxy written in polar coordinates (r, θ), and $u = \ln(r)$. We define the Fourier transform of this image as:

$$A(p, m) = \int_{u_{\min}}^{u_{\max}} \int_0^{2\pi} I(u, \theta) \exp[\mathrm{i}(pu + m\theta)]\, \mathrm{d}\theta \mathrm{d}u. \quad (1)$$

In this equation, p corresponds to the radial frequency and m to the azimuthal frequency. Thus the $m = 1$ values correspond to an asymmetry, the $m = 2$ values to a bisymmetric component, and so on. The values of $u_{\min} = \ln(r_{\min})$ and $u_{\max} = \ln(r_{\max})$ are set by the inner and outer radius of the image, or of the part that we will analyze.

Fixing the value of m, we can calculate the power associated to this component simply as:

$$P_m = |A(p, m)| = \left| \int_{-p_{\max}}^{p_{\max}} A(p, m)\, \mathrm{d}p \right|. \quad (2)$$

The value of $p_{\max}$ is related to the resolution in Fourier space through

$$p_{\max} = \frac{1}{2\Delta u} = \frac{N - 1}{2(u_{\max} - u_{\min})}, \quad (3)$$

where N is the number of points used in the Fourier transform in the radial dimension, usually $N = 256$ or $N = 512$.

In our first method we try to minimize the effect of all non-axisymmetric structure by minimizing the ratio:

$$BAG1 = \frac{P_1 + P_2 + \cdots + P_6}{P_0 + P_1 + \cdots + P_6}. \quad (4)$$

This is equivalent to maximizing the contribution of the axisymmetric component. Experience shows that components of order larger than 6 are too noisy to be of use. Since a badly deprojected galaxy will look oval, and thus contribute to the $m = 2$ component as a bar, for our second method we simply minimize the ratio

$$BAG2 = \frac{P_2}{P_0}. \quad (5)$$

None of the methods proposed so far are free from systematic errors. They are designed to work properly in the case of perfectly axisymmetric thin discs in circular motion about their centers, which is rarely the case for real disc galaxies. For instance, when we try to fit ellipses to the outer isophotes, the presence of strong arms, or (pseudo-) rings can influence the value of the PA, and hence also the IA. This particular bias is known as Stock's effect (1955). On the other hand, warps in the outer parts of the discs, or non-circular motions in the central parts due to bars or other perturbations, can bias the results of the kinematical methods. The methods based on the Fourier analysis of the images are also not free of systematic biases, but their results are as reliable as the kinematical methods, as shown in BAG. Thus, the more reliable way of determining the deprojection angles is to compile the information of different sources and to combine the results in order to minimize the different biases. This is the procedure we followed for the spiral galaxies in the Frei et al. (1996) sample and we will also follow it for the present sample.

3. Application to the OSU sample of galaxies

For each galaxy in the sample we proceed as follows to determine the deprojection angles. First we make a thorough search in the literature of all the determinations of the deprojection angles using different methods. Then we apply the BAG1 and BAG2 methods to each of the images of the galaxies in the sample. The values obtained for each method and each image are averaged to give the results of each of our two methods. We then use the literature values and the values determined by our two methods to deproject the broad band B image of each galaxy. We do not use the H band image, since, sometimes at least, it goes to less depth than the B band image, and since for some galaxies the field of view is too limited. According to the shape of the deprojected image we give a weight to the pair of determined deprojection angles. If the deprojected image is neatly round we give a weight of 3; we diminish the weight as the deprojected image deviates from circular shape. This allows us to spot some systematic errors, as e.g. cases where the photometry does not extend to sufficiently large radii, and thus minimize their effects on the finally adopted value. These weights, together with other information on the quality of the individual studies, considerations on how appropiate a particular method is for the galaxy at hand etc., are taken into account when adopting the final (PA, IA) values.

We checked our results by visual inspection of all the deprojected images. We found that for 35 out of the 158 galaxies (22%) a correction to the value obtained by the weighted average of all results was necessary. Three categories of galaxies were particularly affected : 1) galaxies with strong outer spiral structure or outer (pseudo-) rings, like the galaxies NGC 1350, NGC 5247 and NGC 7479; 2) highly inclined galaxies with a strong bulge, like NGC 3169 and NGC 4856; and 3) galaxies seen very face-on, like NGC 3938 and NGC 4303, for which the determination of the position angle is difficult. For the galaxies in groups 1) and 2), normally a typical correction of $5°-10°$ was necessary, while for very face-on galaxies our methods can give values for the PA quite different from the values determined using other methods. Where adequate, we preferred the determination based on HI kinematics, but in other cases we adopted the criterion that the outer disk isophote has to be circular. This percentage of correction bodes ill for a full automation of the deprojection process in case of very large samples, as becomes possible e.g. with the Sloan Digital Sky Survey.

The results of our analysis are shown in Table 1, which will be published in the electronic version only. In Col. 1 we give the galaxy name, then for each galaxy we give in Cols. 2 and 3 the results of method *BAG*1 for each of the colour bands. Columns 4 and 5 give the results of method *BAG*2. In both cases the colour bands are listed in the sequence B, H. Column 6 gives the colour band used to obtain the image. Columns 7 and 8 give respectively the PA and IA measured for this galaxy using other methods that were found in the literature. Column 9 gives a weight for these values. These were obtained deprojecting the galaxy image in the *B* band, and are just a measure of the degree of roundness of this particular image using these particular values of the deprojection angles. Column 10 gives a code for the deprojection method used to obtain these values. For photometric techniques we use a P, for kinematics we use a K symbol followed by another letter to indicate the kind of kinematics used. Thus, KH indicates HI velocity fields, KO optical two-dimensional velocity fields, KC is used for CO velocity fields and KS for long slit measures. The symbol KP indicates a combination of the information coming from both kinematic and photometric analyses. For methods based on the spiral structure we use a S. In Col. 11 we give a code number to point to the reference from which these values were obtained, which is resolved at the end of the table. In Cols. 12 and 13 we give the mean PA and IA of the values obtained by method *BAG*1 using all the available filters for this galaxy. These mean values are the values that we will use for this galaxy and method *BAG*1. Column 14 gives a weight for these values as in Col. 9. Columns 15–17 give the same values as Cols. 12–14, but for method *BAG*2. Finally, in Col. 18 we give the adopted PA value for this galaxy computed as the weighted mean of all the available values and in Col. 19 the uncertainty in this value of the PA, computed as the weighted dispersion. Columns 20 and 21 give the same values for the adopted IA. In Table 2 we give only the adopted values and their uncertainties for each galaxy. In Col. 1 we give the galaxy name, in Cols. 2 and 3 the adopted PA and its uncertainty ΔPA and in Cols. 4 and 5 the adopted IA and its uncertainty ΔIA.

4. Comparison with data in the literature

Some of the galaxies are present both in the Frei et al. (1996) and the Ohio (2002) samples. We have made a consistency check between the values determined by the BAG methods using different images in different passbands for these galaxies, obtained with different instrumentation.

In order to compare the values obtained using the two samples we fit a straight line to all pairs of values, using a

Table 2. Adopted values of the deprojection angles for the galaxies in the sample.

Name	PA	Δ PA	IA	Δ IA
IC 4444	55	2	34	5
IC 5325	14	13	31	2
NGC 150	119	2	61	3
NGC 157	38	4	46	3
NGC 210	163	5	51	3
NGC 278	39	7	22	4
NGC 289	132	8	41	5
NGC 488	9	4	39	2
NGC 578	107	4	57	4
NGC 613	118	5	44	2
NGC 685	97	–	35	6
NGC 779	160	–	73	2
NGC 864	32	12	43	3
NGC 908	77	2	63	1
NGC 1003	95	1	71	1
NGC 1042	112	–	35	–
NGC 1058	145	–	15	8
NGC 1073	164	–	19	–
NGC 1084	38	6	53	4
NGC 1087	1	2	52	2
NGC 1187	135	6	40	6
NGC 1241	143	3	55	1
NGC 1300	87	–	35	–
NGC 1302	180	1	17	–
NGC 1309	75	6	26	1
NGC 1317	78	–	29	–
NGC 1350	6	6	59	1
NGC 1371	133	2	45	1
NGC 1385	174	5	51	3
NGC 1421	6	7	81	5
NGC 1493	71	2	21	–
NGC 1559	63	1	57	3
NGC 1617	106	1	62	1
NGC 1637	31	–	40	–
NGC 1703	177	–	30	–
NGC 1792	137	2	62	2
NGC 1832	17	11	46	3
NGC 1964	29	3	67	1
NGC 2090	12	2	65	–
NGC 2196	50	8	39	2
NGC 2280	163	–	67	–
NGC 2559	6	–	63	1
NGC 2775	158	3	38	3
NGC 2964	94	2	54	3
NGC 3059	0	–	0	–
NGC 3169	50	3	53	4
NGC 3223	128	4	48	3
NGC 3261	77	14	40	1
NGC 3275	30	–	20	–

Table 2. continued.

Name	PA	ΔPA	IA	ΔIA
NGC 3319	39	2	61	4
NGC 3338	96	3	55	5
NGC 3423	31	14	34	2
NGC 3504	155	–	19	3
NGC 3507	92	11	28	5
NGC 3511	73	2	69	0
NGC 3513	123	9	36	7
NGC 3583	125	2	51	2
NGC 3596	146	8	29	3
NGC 3646	50	2	60	3
NGC 3675	180	–	63	–
NGC 3681	108	3	11	16
NGC 3684	130	5	47	3
NGC 3686	18	6	39	3
NGC 3705	122	–	65	–
NGC 3726	14	2	53	3
NGC 3810	25	5	45	2
NGC 3877	36	1	77	1
NGC 3887	9	7	42	4
NGC 3893	169	5	51	2
NGC 3938	21	1	11	6
NGC 3949	119	2	52	2
NGC 4030	32	6	40	2
NGC 4051	132	2	43	5
NGC 4062	99	2	66	2
NGC 4100	167	2	72	1
NGC 4123	132	7	48	5
NGC 4136	97	8	31	7
NGC 4145	101	8	55	–
NGC 4151	21	1	21	1
NGC 4178	33	2	72	2
NGC 4212	74	1	52	3
NGC 4254	59	3	29	5
NGC 4303	137	1	27	–
NGC 4314	79	14	26	2
NGC 4388	90	2	74	4
NGC 4394	111	4	25	3
NGC 4414	160	4	54	4
NGC 4448	93	1	67	1
NGC 4450	175	5	51	4
NGC 4457	82	–	31	–
NGC 4487	76	6	52	3
NGC 4504	143	2	51	2
NGC 4527	68	2	70	2
NGC 4548	141	5	35	11
NGC 4571	42	8	32	3
NGC 4579	94	4	37	2
NGC 4580	159	5	43	4

Table 2. continued.

Name	PA	ΔPA	IA	ΔIA
NGC 4593	98	16	46	2
NGC 4618	23	10	38	4
NGC 4643	58	11	37	4
NGC 4651	78	5	48	2
NGC 4654	122	3	57	4
NGC 4665	115	3	29	2
NGC 4666	41	–	74	1
NGC 4689	162	5	36	4
NGC 4698	168	–	67	–
NGC 4699	45	2	43	3
NGC 4772	145	1	65	2
NGC 4775	93	–	18	–
NGC 4781	117	4	62	2
NGC 4818	0	–	72	–
NGC 4900	0	–	18	–
NGC 4902	102	21	23	7
NGC 4930	55	9	40	4
NGC 4939	8	5	59	3
NGC 4941	17	1	59	2
NGC 4995	96	3	47	2
NGC 5005	65	–	63	–
NGC 5054	159	2	54	1
NGC 5085	39	9	38	7
NGC 5101	140	–	32	–
NGC 5121	27	5	35	2
NGC 5161	78	1	66	1
NGC 5247	22	14	24	5
NGC 5334	15	3	43	5
NGC 5371	8	–	46	5
NGC 5427	72	6	32	6
NGC 5448	108	4	66	3
NGC 5483	21	5	26	3
NGC 5643	108	2	23	0
NGC 5676	46	1	61	1
NGC 5701	45	–	20	–
NGC 5713	12	2	30	2
NGC 5850	160	11	34	4
NGC 5921	137	10	36	3
NGC 5962	109	4	45	2
NGC 6215	78	–	34	–
NGC 6221	178	6	50	7
NGC 6300	115	6	50	1
NGC 6384	32	4	48	2
NGC 6753	29	4	34	3
NGC 6782	45	–	26	2
NGC 6902	155	1	45	3
NGC 6907	45	1	32	3
NGC 7083	5	1	58	4

Table 2. continued.

Name	PA	ΔPA	IA	ΔIA
NGC 7184	62	1	73	2
NGC 7205	69	3	60	1
NGC 7213	30	7	15	2
NGC 7217	86	5	29	4
NGC 7412	45	–	42	–
NGC 7418	137	2	40	3
NGC 7479	35	7	44	4
NGC 7552	175	7	38	5
NGC 7582	157	–	65	–
NGC 7606	146	–	68	–
NGC 7713	172	3	68	–
NGC 7723	41	8	47	1
NGC 7741	166	4	43	5

maximum likelihood algorithm (Press et al. 1992), which minimizes the χ^2 merit function

$$\chi^2(a,b) = \sum_{i=1}^{N} \frac{(y_i - a - bx_i)^2}{\sigma_{yi}^2 + b^2\sigma_{xi}^2}, \qquad (6)$$

where σ_{xi}^2 and σ_{yi}^2 are a measure of the errors for the ith value.

In the correlations including the PA, we assign weights according to the IA, since galaxies with low inclination have ill-defined position angles. These weights are taken from a linear function of the IA, such that this weight is zero for a face on galaxy (IA = 0) and unity for a galaxy with IA ≥ 30 degrees. For IA ≥ 30 this weight is taken as unity. The σ_{xi} and σ_{yi} appearing in Eq. (6) are defined as the inverse of the weights, i.e $\sigma_i = 1/w_i$. For the correlations with the IA we use unweighted values, i.e. $\sigma_{xi} = \sigma_{yi} = 1$.

The comparison (not shown here) between the values of the BAG1 method derived for the galaxies in the Frei sample and those in the Ohio sample is excellent, the correlation coefficient of the PA values is 0.97, and for the case of the cos (IA) values is 0.98. In the case of the BAG2 method the correlation coefficient is 0.96 for the PA values and 0.94 for the cos (IA) values. These values indicate that our methods give comparable values when used on images taken from different samples and with different passbands. Thus, this is a further indication of the robustness of our two methods, which, added to the relative comparison with the other methods presented in BAG, shows that our methods can be used with confidence.

We also compared the results for our methods with data from the RC3, and with kinematic data available in the literature. We show in Figs. 1 and 2 the comparison with BAG2. Results for BAG1 are similar and thus will not be shown here. In Fig. 1, the correlation coefficient is 0.96 for the PA values, and 0.87 for the cos (IA) values. The three outlying points above the correlation in the left panel of Fig. 1 correspond to three late spirals with a very open spiral structure while in the inner parts there is a late type bar.

As for the comparison with the kinematic data, in Fig. 2, the correlation coefficient is 0.84 for the PA values, and 0.85 for the cos (IA) values. There is thus a good correlation, but not an excellent one. Excluding the galaxies for which the inclination is less than IA = 30 degrees, the correlation improves significantly. The correlation coefficients now become 0.96 and 0.88 for the PA and the cos (IA), respectively. This reflects the fact that for galaxies not far from face-on only the kinematics can provide a good estimate for the deprojection angles. It also argues that our methods fare very well for all galaxies which are not nearly face-on.

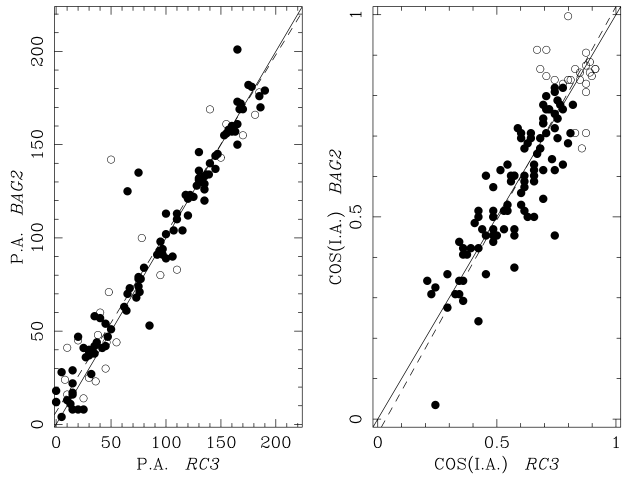

Fig. 1. Comparison of the deprojected angles obtained with *BAG*2 with RC3 values, for the galaxies present in the Ohio sample. Left panel corresponds to the correlation for the PA values, while the right panel shows the correlation for the cos (IA) values. Galaxies with inclination less than 30 degrees are plotted with open symbols and the remaining ones with full symbols. The solid line gives the least squares fitting straight line, calculated as explained in the text, and the dashed one the diagonal.

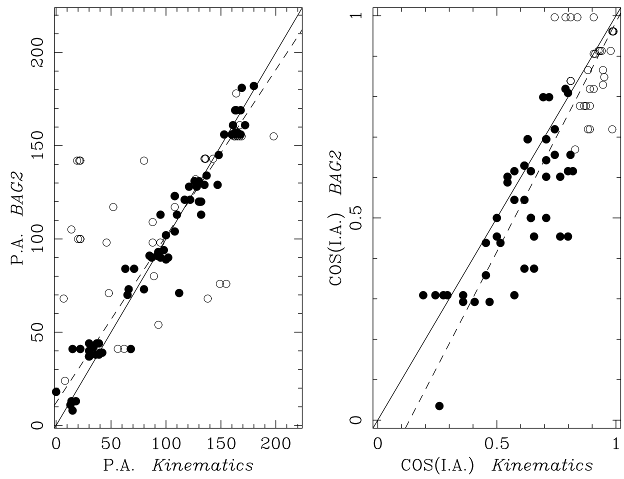

Fig. 2. Comparing the deprojected angles obtained with *BAG*2 for the galaxies in the Ohio sample with data obtained from kinematics in the literature. The layout is as in Fig. 1.

5. Summary

In this paper we calculate the deprojection angles of the spiral galaxies in the Ohio State University Bright Galaxy Sample. These values are determined using all the information compiled in the literature, plus the results of two methods based on the Fourier analysis of galaxy images developed recently by some of the authors (BAG). We thus provide a homogeneous set of values for the deprojection angles, a necessary first step for a number of statistical studies of disc galaxy properties.

We have also compared the results of BAG1 and BAG2 with data from RC3 and with estimates from large scale kinematics found in the literature, and find that our methods perform very well, except for cases where the galaxy is nearly face-on, where only the estimates from kinematics are reliable.

Our methods, as well as most of the other ones, rely on two assumptions, which, if found to be considerably wrong could introduce a significant bias. The first assumption is that the galactic discs are thin. Although corrections for thickness are possible, as e.g. advocated in the RC3, they are rather cumbersome, have to rely on statistical evaluations and can also introduce some bias. The second assumption is that discs are not oval. The question of noncircular disks is not an easy one to settle on a statistical basis, as indicated by recent work by Ryden (2004). If discs are indeed found to be oval, then the result of *all* deprojection methods will be flawed and several results on galactic discs will need to be revised. This will also have considerable implications on the density distribution in galactic halos. Discussing them, or divising new methods which can find the orientation parameters for such disk galaxies is beyond the scope of this paper.

From the discussion in the previous sections we can conclude that our two methods fare at least as well as other deprojection methods, but that the best approach is to compile results from different methods and use them all to obtain the values of the orientation parameters. Of course this is lengthy and will be difficult to do for large samples, such as the ones that can be obtained from the Sloan Digital Sky Survey.

Acknowledgements. We thank the referee, R. Buta for his helpful suggestions which improved considerably the present paper. We thank also Guiseppe Aronica for his help in the initial stages of the image cleaning. In preparing this paper we made extensive use of the CDS Strasbourg database. C.G.G. and C.B. acknowledge financial support by the Dirección de Investigación cintífica y Técnica under contract AYA2001-0762. We also thank the Picasso program of bilateral exchanges under contract HF2001-023, and support from the European Union under contract HPMT-CT-2001-00338.

References

Aguerri, J. A. L., Varela, A. M., Prieto, M., & Muñoz-Tuñón, C. 2000, AJ, 119, 1638
Allsopp, N. J. 1979, MNRAS, 188, 765
Alonso-Herrero, A., Simpson, Ch., Ward, M. J., & Wilson, A. S. 1998, ApJ, 495, 196
Barberà, C., Athanassoula, E., & García-Gómez, C. 2004, A&A, 415, 849
Baumgart, C. W., & Peterson, C. J. 1986, PASP, 98, 56
Becker, R., Mebold, U., Reif, K., & van Woerden, H. 1988, A&A, 203, 21
Bertola, F., Corsini, E. M.,Vega Beltrán, J. C., et al. 1999, ApJ, 519, 127
Blackman, C. P. 1979a, MNRAS, 186, 701
Blackman, C. P. 1979b, MNRAS, 186, 717
Blackman, C. P. 1979c, MNRAS, 188, 93
Blackman, C. P. 1980a, MNRAS, 190, 459
Blackman, C. P. 1980b, MNRAS, 191, 123
Blackman, C. P. 1981, MNRAS, 195, 451
Blackman, C. P. 1982, MNRAS, 198, 517
Blackman, C. P. 1983, MNRAS, 202, 379
Boroson, T. A. 1981, ApJS, 46, 177
Boroson, T. A., Strom, K. M., & Strom, S. E. 1983, ApJ, 274, 39
Bosma, A., Ekers, R. D., & Lequeux, J. 1977, A&A, 57, 97
Boselli, A., Lequeux, J., Contursi, A., et al. 1997, A&A, 324, 13
Broeils, A. H., & van Woerden, H. 1994, A&AS, 107, 129
Burbidge, E. M., & Burbidge, G. R. 1968, ApJ, 154, 857
Burbidge, E. M., Burbidge, G. R., & Prendergast, K. H. 1960, ApJ, 132, 654
Burbidge, E. M., Burbidge, G. R., & Prendergast, K. H. 1961, ApJ, 134, 874
Burbidge, E. M., Burbidge, G. R., & Prendergast, K. H. 1963, ApJ, 138, 375
Buta, R. 1987, ApJS, 64, 383
Buta, R., van Driel, W., Braine, J., et al. 1995, ApJ, 450, 593
Comte, G., Monnet, G., & Rosado, M. 1979, A&A, 72, 73
Considère, S., & Athanassoula, E. 1982, A&A, 111, 82
Considère, S., & Athanassoula, E. 1988, A&AS, 76, 365
Crocker, D. A., Baugus, P. D., & Buta, R. 1996, ApJS, 105, 353
Dahlem, M. 1992, A&A, 264, 483
Danver, C. G. 1942, Lund. Obs. Ann., No. 10
de Jong, R. S., & van der Kruit, P. C. 1994, A&AS, 106, 451
de Vaucouleurs, G., de Vaucouleurs, A., Corwin, H. G., et al. 1991, Third Reference Catalogue of Bright Galaxies (New York: Springer) (RC3)
Duval, M. F. 1983, IAUS, 100, 237
Duval, M. F., & Monnet, G. 1985, A&AS, 61, 141
England, M. N. 1989, ApJ, 344, 669
England, M. N., Gottesman, S. T., & Hunter, J. H. Jr. 1990, ApJ, 348, 456
Erwin, P., & Sparke, L. S. 2003, ApJS, 146, 299
Eskridge, P. B., Frogel, J. A., Pogge, R. W., et al. 2002, ApJS, 143, 73
Foster, P. A., & Nelson, A. H. 1985, MNRAS, 215, 555
Frei, Z., Guhathakurta, P., Gunn, J., & Tyson, J. A. 1996, AJ, 111, 174
Fridman, A. M., Khorizhii, O. V., Lyakhovich, V. V., et al. 2001, A&A, 371, 538
Gallimore, J. F., Baum, S. A., O'Dea, C. P., Pedlar, A., & Brinks, E. 1999, ApJ, 524, 684
García-Gómez, C., & Athanassoula, E. 1991, A&AS, 89, 159
García-Gómez, C., Athanassoula, E., & Barberá, C. 2002, A&A, 389, 68
Garrido, O., Marcelin, M., Amram, P., & Boulesteix, J. 2002, A&A, 387, 821
Grosbøl, P. J. 1980, in Photometry and Kinematics of Galaxies, 101
Grosbøl, P. J. 1985, A&AS, 60, 261
Grosbøl, P. J., & Patsis, P. A. 1998, A&A, 336, 840
Guhatakurta, P., van Gorkom, J. H., Kotany, C. G., & Balkowski, C. 1988, AJ, 96, 851
Haynes, M. P., Giovanelli, R., Chamaraux, P., et al. 1999, AJ, 117, 2093
Haynes, M. P., Jore, K. P., Barrett, E. A., Broelis, A. H., & Murray, B. M. 2000, AJ, 120, 703
Héraudeau, Ph., & Simien, F. 1996, A&AS, 118, 111
Higdon, J. L., Buta, R. J., & Purcell, G. B. 1998, AJ, 115, 80
Hunt, L. K., Malkan, M. A., Rush, B., et al. 1999, ApJS, 125, 349
Iye, M., Okamura, S., Hamabe, M., & Watanabe, M. 1982, ApJ, 256, 103
Irwin, J. A., English, J., & Sorathia, B. 1999, AJ, 117, 2102

Jarrett, T. H., Chester, T., Cutri, R., Schneider, S. E., & Huchra, J. P. 2003, AJ, 125, 525
Kaneko, N., Aoki, K., Kosugi, G., et al. 1997, AJ, 114, 94
Kenney, J. D. P., Carlstrom, J. E., & Young, J. S. 1993, ApJ, 418, 687
Kent, S. 1986, AJ, 91, 130
Kent, S. 1988, AJ, 96, 514
Kornreich, D. A., Hayes, M. P., Lovelace, R. V. E., & van Zee, L. 2000, AJ, 120, 139
Koopmann, R. A., Kenney, J. D. P., & Young, J. 2001, ApJS, 135, 125
Laine, S., & Gottesman, S. T. 1998, MNRAS, 297, 1052
Lindblad, P. A. B., Kristen, H., Joersaeter, S., & Hoegbom, J. 1997, A&A, 317, 36
Lu, N. Y. 1998, ApJ, 506, 673
Ma, J., Peng, Q.-H., & Gu, Q.-S. 1998, A&AS, 130, 449
Ma, J. 2001, ChJAA, 1, 395
Mathewson, D. S., & Ford, V. L. 1996, ApJS, 107, 97
Miller, B., & Hodge, P. W. 1991, BAAS, 23, 966
Moiseev, A. V. 2000, A&A, 363, 843
Möllenhoff, C., & Heidt, J. 2001, A&A, 368, 16
Moore, E. M., & Gottesman, S. T. 1998, MNRAS, 294, 353
Moriondo, G., Giovanardi, C., & Hunt, L. K. 1988, A&AS, 130, 81
Odewahn, S. C. 1991, AJ, 101, 829
Ohta, K., Hamabe, M., & Wakamatsu, K. 1990, ApJ, 357, 71
Okamura, S. 1978, PASJ, 30, 91
Oosterloo, T., & Shostak, S. 1993, A&AS, 99, 379
Pedlar, A., Howley, P., Axon, D. J., & Unger, S. W. 1992, MNRAS, 259, 369
Peletier, R. F., Knapen, J. H., Shlosman, I., et al. 1990, ApJS, 125, 409
Peletier, R. F., & Willner, S. P. 1991, ApJ, 382, 382
Pellet, A., & Simien, F. 1982, A&A, 106, 214
Pence, W. D., & Blackman, C. P. 1984a, MNRAS, 207, 9
Pence, W. D., & Blackman, C. P. 1984b, MNRAS, 210, 547
Peterson, C. J., & Huntley, J. M. 1980, ApJ, 242, 913
Phookun, B., Vogel, S. N., & Mundy, L. G. 1993, ApJ, 418, 113
Press, W. H., Teukolsky, S. A., Vetterling, W. H., & Flannery, B. P. 1992, Numerical Recipes (Cambridge Univ. Press.)
Prieto, M., Longley, D. P. T., Pérez, E., et al. 1992, A&AS, 93, 557
Prieto, M., Gottesman, S. T., Aguerri, J. A. L., & Varela, A. M. 1997, AJ, 114, 1413
Rhee, M.-H., & van Albada, T. S. 1996, A&AS, 115, 407
Rots, A. H. 1980, A&AS, 41, 189
Rubin, V. C., Burbidge, E. M., Burbidge, G. R., & Prendergast, K. H. 1964, ApJ, 140, 80
Rubin, V., Waterman, A. H., & Kenney, J. D. P. 1999, AJ, 118, 236
Ryden, B. S. ApJ, 601, 214
Ryder, S. D., Buta, R. J., Toledo, H., et al. 1996, ApJ, 460, 665
Ryder, S. D., Zasov, A. V., Sil'chenki, O. K., McIntyre, V. J., & Walsh, W. 1988, MNRAS, 293, 338
Sánchez-Portal, M., Díaz, A. I., Terlevich, R., et al. 2000, MNRAS, 312, 2
Schmitt, M., & Kinney, A. L. 2000, ApJS, 128, 479
Sperandio, M., Chincarini, G., Rampazzo, R., & de Souza, R. 1995, A&AS, 110, 279
Sofue, Y., Tomita, A., Honma, M., & Tutui, Y. 1999, PASJ, 51, 737
Stock, J. 1955, AJ, 60, 216
Swaters, R. A., & Balcells, M. 2002, A&A, 390, 863
Terndrup, D. M., Davies, R. L., Frogel, J. A., DePoy, D. L., & Wells, L. A. 1994, ApJ, 432, 518
Tully, B., Verheijen, M. A. W., Pierce, M. J., Huang, J. S., & Wainscoat, R. J. 1996, AJ, 112, 247
van der Kruit, P. C., & Shostak, G. S. 1982, A&A, 105, 351
van Moorsel, G. A., & Wells, D. C. 1985, AJ, 90, 1038
Verheijen, M. A. W., & Sancisi, R. 2001, A&A, 370, 765
Vollmer, B., Cayate, V., Boselli, A., Balkowski, C., & Duschl, W. J. 1999, A&A, 349, 411
Walsh, W., Staveley-Smith, L., & Oosterloo, T. 1997, AJ, 113, 1591
Warmels, R. H. 1998a, A&AS, 72, 427
Warmels, R. H. 1998b, A&AS, 73, 453
Weiner, B. J., Williams, T. B., van Gorkom, J. H., & Sellwood, J. A. 2001, ApJ, 546, 916
Wevers, B. M. H. R., van der Kruit, P. C., & Allen, R. J. 1986, A&AS, 66, 505
Zasov, A. V., & Kyazumov, G. A. 1981, Sov. Astron. Lett., 7, 73